Check for updates

Benchmarking acetylthiophene derivatives: methyl internal rotations in the microwave spectrum of 2-acetyl-5-methylthiophene†

Christina Dindić[a] and Ha Vinh Lam Nguyen ![ID] ★[bc]

The microwave spectrum of 2-acetyl-5-methylthiophene (2A5MT) was recorded using a molecular jet Fourier transform microwave spectrometer working in the frequency range of 2 to 26.5 GHz. The spectrum was assigned to the *syn*-conformer of the molecule while that of *anti*-2A5MT was not observable. For the assignment of the spectrum of 2A5MT, adequate spectral analysis skill and quantum chemical benchmarking helped to significantly reduce the time required for recording survey scans. The rotational and centrifugal distortion constants were determined with high accuracy. The experimental values of the rotational constants are compared to those derived from quantum chemical calculations in the course of ongoing benchmarking effort. Splitting of each rotational transition into quintets due to internal rotations of the acetyl methyl and ring methyl groups could be resolved and analysed to yield barriers to internal rotations of 301.811(41) cm^{-1} and 157.2612(13) cm^{-1}, respectively. These values are compared to those found in other thiophene and furan derivatives in order to understand the electronic effects transmitted through aromatic rings, as well as how different heteroatoms affect torsional barriers. The acetyl methyl group features torsional barriers of around 300 cm^{-1} if a thiophene derivative is attached at the other side of the carbonyl group. This finding allows the establishment of the so-called "thiophene class" for the acetyl group containing ketones.

1. Introduction

Almost a century ago, torsion oscillator rotation was treated for the first time quantum mechanically by Nielsen in 1932.[1] Four years later, from calorimetric measurements, Kemp and Pitzer stated that the methyl torsion in ethane is hindered by a potential barrier, which opened up a new research subject on internal rotation.[2] A significant number of studies on molecules containing one or more methyl rotors have been performed, but the barrier and its origin have not been fully understood yet from both experimental and theoretical perspectives.[3–7] However, it is known that the height and shape of the torsional potential depend on the conformation of the molecule and the intramolecular interactions. Today, the method probably most accurate to determine the barrier to internal rotation is molecular jet Fourier transform microwave (FTMW) spectroscopy.[8–10] Appropriate Hamiltonians accounting for the internal rotation

of a methyl group attached onto an asymmetrical frame have been developed using several program codes such as BELGI-C$_s$,[11] BELGI-C$_1$,[12] RAM36[13] and aixPAM[14] for one-top molecules, ERHAM[15] for up to two-top molecules, BELGI-C$_s$-2Tops[16] and PAM-C$_{2v}$-2tops[17] for two-top molecules, XIAM[18] for up to three-top molecules and *n*top for *n*-top molecules[19] (currently tested at *n* = 4) to solve many internal rotation problems. Nevertheless, analysing the microwave spectra of molecules with multiple methyl rotors (*n* > 1) is still challenging due to their complexity. If in one-top molecules, A–E torsional doublets are observed for each rotational transition, they appear as quintets in two-top molecules if the rotors are inequivalent. The quintet components are called $(\sigma_1\sigma_2)$ = (00), (01), (10), (11) and (12) species,[20] corresponding to the A, E1, E2, E3 and E4 species, respectively, using the permutation–inversion formalism of the G$_{18}$ group[21] or to the AA, AE, EA, EE and EE* species in Dreizler's notation.[22] The number of torsional components in the multiplets increases rapidly with the number of rotors present in the molecules.[9] With the rapid development of quantum chemical calculations to compute not only the molecular geometries but also the torsional potentials with sufficient accuracy over last few decades, quantum chemistry has become a powerful supporting tool for FTMW spectroscopy to face challenges in analysing spectra with internal rotations.

^{a} *Institute of Physical Chemistry, RWTH Aachen University, Landoltweg 2, D-52074 Aachen, Germany*

^{b} *Univ Paris Est Creteil and Université de Paris, CNRS, LISA, F-94010 Créteil, France. E-mail: lam.nguyen@lisa.ipsl.fr*

^{c} *Institut Universitaire de France (IUF), F-75231 Paris cedex 05, France*

† Electronic supplementary information (ESI) available. See DOI: https://doi.org/10.1039/d2cp03897h

This journal is © the Owner Societies 2023

Phys. Chem. Chem. Phys., 2023, **25**, 509–519 | **509**

The FTMW results on 2-acetyl-3-methylthiophene (2A3MT)[23] and 2-acetyl-4-methylthiophene (2A4MT)[24] have been recently published. To further examine the effects of multiple methyl internal rotations, it was natural to continue with the two-top molecule 2-acetyl-5-methylthiophene (2A5MT), which is the last one in a series of 2-acetylmethylthiophenes. From our investigations on 2A3MT and 2A4MT and many further molecules,[25–28] it is known that steric and electrostatic effects are the two main factors affecting the torsional barriers. In *n*-alkyl acetates, the same value of about 100 cm^{-1} is observed for the barrier to the internal rotation of the acetyl methyl group in different conformers.[9,29,30] The value increases to 135 cm^{-1} or 150 cm^{-1} in α,β-unsaturated acetates.[31–34] In *tert*-butyl acetates, the bulky *tert*-butyl group augments the methyl torsional barrier from 100 cm^{-1} to 111 cm^{-1}.[35] We were interested in exploring the torsional barriers in 2A5MT, and comparing them with the values found for 2A3MT[23] and 2A4MT[24] as well as related molecules to better understand the steric and electrostatic effects in thiophene containing molecules with methyl internal rotation(s).[36] For aliphatic ketones containing an acetyl group CH$_3$–CO, Andresen *et al.* proposed a classification to link the barrier height of the acetyl methyl group CH$_3$– to the molecular structure.[37,38] Linear aliphatic ketones were categorised into two classes: the C$_1$ class with a barrier of about 240 cm^{-1} and the C$_s$ class with a barrier of approximately 180 cm^{-1}.[37,39–41] α,β-Unsaturated ketones were grouped in the "mesomeric class" containing two sub-classes: antiperiplanar (ap) with a barrier of about 430 cm^{-1} and synperiplanar (sp) with a barrier of 350 cm^{-1}.[38] The categorisation was extended by Herbers *et al.* with the "phenyl class".[42] With data points from 2-acetylthiophene, 2A3MT, and 2A4MT, we proposed a "thiophene class" considering the torsional barriers of acetyl methyl groups in ketones which contain a thiophene ring on the other side of the carbonyl bond.[24] The results of 2A5MT in the present work yielded a further important data point to establish this thiophene class. We will also compare the barrier height of the methyl top attached to the thiophene ring with that of methylthiophene and methylfuran derivatives to discuss the influence of the heteroatom in the aromatic ring on the methyl torsional barrier.

A classic resonator-based FTMW spectrometer was available for the investigation of 2A5MT, which is known for its high resolution but suffers from the time requirement for survey spectra. However, this drawback can be circumvented with the help of adequate spectral assignment skill and knowledge gained from quantum chemical benchmarking. From benchmarks on the rotational constants of the isomers 2A3MT[23] and 2A4MT,[24] it is known that the equilibrium rotational constants calculated at the MP2/6-31G(d,p) level of theory are very close to the experimentally determined values. With this gained knowledge, it can be inferred that only very small scan portions around the predicted frequencies of some transitions are needed. Furthermore, the benchmarks on 2A5MT also include the methyl torsional barriers of both methyl rotors. Predicting torsional barriers is challenging. Unlike for molecular geometries, benchmarking barriers to methyl internal rotation is only at an early stage due to the cost of the calculations.[43] Recently, we have also started to benchmark the barrier heights of 2-acetylmethylthiophenes in our investigations on 2A3MT and 2A4MT, using the same levels used for benchmarking the molecular geometries, and we have continued this effort also for 2A5MT.

2. Quantum chemical calculations

2.1. Conformational analysis

Since the thiophene ring is planar,[44] the acetyl group is the only moiety in 2A5MT whose orientation changes create different conformers. In previous investigations on similar molecules containing an acetyl group, such as 2-acetylthiophene,[45] 2A3MT[23] and 2A4MT,[24] only two conformers are possible with the oxygen atom of the acetyl group being either in an *anti* or in a *syn* orientation relative to the sulphur atom. Therefore, the same situation is expected for 2A5MT. To analyse the conformational landscape, the dihedral angle α = ∠(S1–C2–C6=O7) (for atom numbering see Fig. 1) was varied in 10° steps, while all other geometry parameters were optimised at the MP2/6-31G(d,p)[46,47] level of theory using the Gaussian 16 program package.[48] This level was chosen from our previous benchmarking experiences,
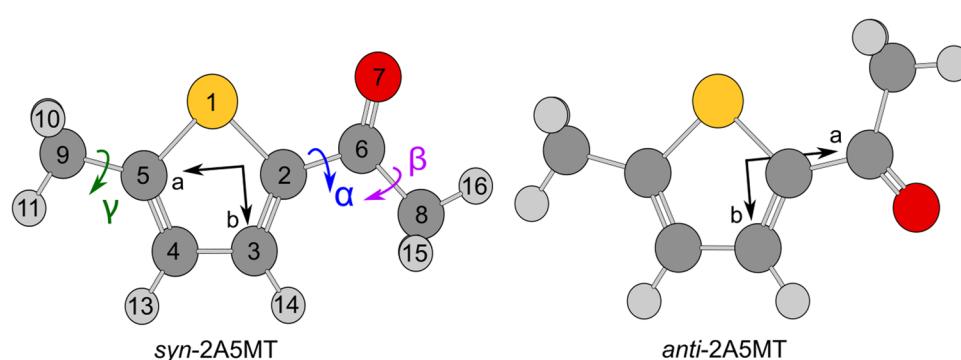
Fig. 1 Geometries of the two conformers of 2A5MT (*syn* and *anti*) optimised at the MP2/6-31G(d,p) level of theory in the principal axes of inertia. Atom numbering and the dihedral angles α = ∠(S1–C2–C6=O7), β = ∠(O7–C6–C8–H16) and γ = ∠(S1–C5–C9–H10) are defined for *syn*-2A5MT. The sulphur atom is marked in yellow, the oxygen atom is marked in red, carbon atoms are marked in dark grey and hydrogen atoms are marked in light grey. H12 lies behind H10, H17 behind H15.

510 | *Phys. Chem. Chem. Phys.*, 2023, **25**, 509–519

This journal is © the Owner Societies 2023
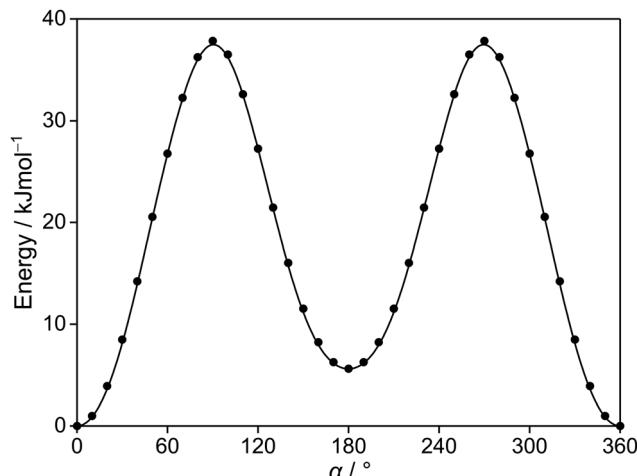
Fig. 2 The potential energy curve of 2A5MT obtained by rotating the acetyl group about the C2–C6 bond (for atom numbering see Fig. 1). The calculations were performed at the MP2/6-31G(d,p) level of theory by varying the dihedral angle α in a grid of $10°$. The relative energies are given with respect to the lowest energy conformation with E_{MP2} = -743.3683072 hartree.

Table 1 Rotational constants, dipole moment components, dihedral angles and relative energies for the two conformers of 2A5MT calculated at the MP2/6-31G(d,p) level of theory

Par.	Unit	syn	anti
A_e	MHz	3425.2	3356.6
B_e	MHz	927.6	928.8
C_e	MHz	736.6	734.1
$|\mu_a|$	D	2.33	3.55
$|\mu_b|$	D	3.87	1.58
$|\mu_c|$	D	0.00	0.00
α	°	0.00	180.00
β	°	0.00	0.00
γ	°	179.86	179.98
ΔE^a	kJ mol^{-1}	0.0	5.3

^{a} Energy differences including zero-point corrections relative to the more stable conformer syn-2A5MT with $E = -743.2336782$ hartree.

as it predicted rotational constants that were very close to the experimentally determined ones for 2A3MT[23] and 2A4MT,[24] the two isomers of 2A5MT. The energy points obtained from these calculations were parameterised with a Fourier expansion using the coefficients given in Table S1 in the ESI.† The resulting potential energy curve shown in Fig. 2 shows that 2A5MT indeed possesses the two expected conformers, which correspond to the minima at $\alpha = 0°$ (syn-2A5MT) and $\alpha = 180°$ (anti-2A5MT). Subsequent full structure optimisations and frequency calculations confirmed both conformers (shown in Fig. 1) to be stable. The calculated rotational constants, dipole moment components, dihedral angles and energy differences between the two conformers are given in Table 1. The atomic coordinates of both the conformers are given in Table S2 in the ESI.†

2.2. Basis set variations

In addition to the MP2/6-31G(d,p) level of theory, we also optimised the structure of the more stable conformer syn-2A5MT using

various method/basis set combinations. The theoretical results are compared with the highly accurate set of rotational constants deduced from the experimental spectrum. This so-called basis set variation is a part of our benchmarking efforts to find the levels of theory allowing for cost-efficient, yet reasonably accurate predictions of rotational constants to guide the assignment of microwave spectra. In the present study, the basis set variation is a confirmation for the fruitful results of our previous benchmarks. Several exchange-correlation functionals from density functional theory (DFT) were selected, such as B3LYP[49,50] with Grimme's distortion corrections[51] and with or without Becke-Johnson damping[52] as well as with the Coulomb-attenuating method (CAM-B3LYP),[53] Truhlar's M06-2X,[54] Head-Condon's ωB97X-D,[55] as well as the ab initio Møller-Plesset perturbation theory of second order (MP2)[46] and the coupled cluster (CCSD) methods.[56] They are combined with different Pople[47] and Dunning[57] basis sets. The results of syn-2A5MT are summarized in Table S3 in the ESI.† An extract of Table S3 (ESI†) is shown in Table 2. For comparison, the corresponding tables for the two isomers 2A3MT[23] and 2A4MT[24] are also given in Table S3 (ESI†).

2.3. Methyl internal rotations

2A5MT possesses two inequivalent internal rotors, the acetyl methyl group and the ring methyl group. We expect the splitting of all rotational transitions into five torsional components $(\sigma_1\sigma_2)$ = (00), (01), (10), (11), and (12).[20] In order to predict the barriers to internal rotations, the respective dihedral angles $\beta = \angle(O7–C6–C8–H16)$ and $\gamma = \angle(S1–C5–C9–H10)$ were varied in $10°$ steps while all other geometry parameters were optimised at the MP2/6-31G(d,p) level of theory. The resulting potential energy curves of syn-2A5MT are shown in Fig. 3, and those of anti-2A5MT are shown in Fig. S1 in the ESI.† The Fourier coefficients utilised to plot the curves are given in Table S4 in the ESI.† We found the typical threefold symmetry expected for methyl groups in all cases. The predicted torsional barriers of syn-2A5MT are 359.0 cm^{-1} and 165.5 cm^{-1} for the acetyl methyl and the ring methyl groups, respectively. The torsional barriers of both rotors were also calculated for syn-2A5MT at all levels used for the geometry optimisations. The predicted values are included in Table 2 and Table S3 (ESI†). Fig. 3 also shows that the other rotor oscillates with an angle of less than $1°$, indicating no coupling between the two rotors. The acetyl oscillation frequently observed in similar molecules[23,24,45] is also absent.

To check whether the coupling between the two rotors can be neglected, a two-dimensional potential energy surface (2D-PES) depending on the dihedral angles β and γ was calculated for syn-2A5MT, again at the MP2/6-31G(d,p) level of theory, in order to study the top–top interaction. Due to the symmetry, only data points in the range from $0°$ to $120°$ were necessary for both β and γ. The potential energies were parameterised with a Fourier expansion with the coefficients listed in Table S5 in the ESI.† The resulting 2D-PES is given in Fig. 4. We only achieved a deviation of 8.0% by fitting the data set but adding cross-coupling coefficients did not enhance the fit, since the values for these terms were negligibly small. Therefore, although the minima are slightly distorted and not circular as in the case of

This journal is © the Owner Societies 2023

Phys. Chem. Chem. Phys., 2023, **25**, 509–519 | 511

Table 2 The deviations between the calculated and the experimental values of the rotational constants ΔA, ΔB and ΔC (calc.−expt., in MHz) of *syn*-2A4MT optimised at various levels of theory, as well as those of the $V_{3,1}$ barrier of the acetyl methyl group and the $V_{3,2}$ of the ring methyl group (expt.−calc., in cm^{-1}). All optimisations were performed under full-symmetry relaxation

Level of theory	ΔA	ΔB	ΔC	$\Delta V_{3,1}$	$\Delta V_{3,2}$	ΔA	ΔB	ΔC	$\Delta V_{3,1}$	$\Delta V_{3,2}$
B3LYP-D3						**M06-2X**				
6-31G(d,p)	−29.3	−8.6	−7.1	19.3	−62.2	0.7	0.4	0.0	−33.5	−48.4
6-31++G(d,p)	−31.7	−11.6	−9.0	86.9	−58.0	−0.7	−1.9	−1.5	24.5	−46.7
6-311G(d,p)	−16.5	−7.3	−5.6	28.9	−39.0	11.0	1.3	1.1	−38.4	−31.1
6-311++G(d,p)	−17.0	−8.9	−6.7	74.7	−52.1	11.1	−0.1	0.2	−4.8	−49.9
cc-pVDZ	−42.0	−10.3	−8.6	−33.1	−38.4	−9.0	−0.8	−1.1	−61.0	−29.5
aug-cc-pVDZ	−39.0	−12.5	−9.9	65.8	−37.8	−6.3	−2.8	−2.3	4.5	−31.6
cc-pVTZ	4.6	−4.1	−2.7	47.4	−14.8	29.1	4.3	3.8	−22.8	−10.0
aug-cc-pVTZ	5.0	−4.4	−2.9	63.8	−11.9	29.9	4.1	3.6	−14.7	−12.0
B3LYP-D3BJ						**MP2**				
6-31G(d,p)	−28.9	−5.2	−4.9	52.8	−43.1	−22.4	0.6	−0.9	−57.2	−8.2
6-31++G(d,p)	−30.9	−8.1	−6.8	122.0	−39.2	−28.1	−2.1	−2.9	39.6	−36.9
6-311G(d,p)	−15.2	−3.9	−3.4	62.4	−19.2	−25.0	−0.6	−1.7	−45.5	−15.5
6-311++G(d,p)	−16.3	−5.4	−4.4	110.3	−32.3	−26.1	−2.5	−3.0	11.0	−44.8
6-311G(df,pd)	−4.0	−1.6	−1.5	73.5	−17.6	1.1	4.6	2.7	−24.9	−19.9
6-311++G(df,pd)	−4.2	−3.0	−2.4	125.8	−20.7	−1.9	2.8	1.5	31.2	−36.9
6-311G(2d,2p)	1.1	−1.0	−0.9	42.5	9.5	−13.7	1.9	0.3	−39.0	24.9
6-311++G(2d,2p)	−0.2	−1.9	−1.5	97.4	3.9	−15.1	0.7	−0.5	13.9	18.7
6-311G(2df,2pd)	8.7	0.8	0.6	39.6	22.6	3.2	7.6	4.7	−34.0	40.5
6-311++G(2df,2pd)	7.7	−0.4	−0.2	93.6	15.1	1.2	6.0	3.6	20.2	29.4
6-311G(3df,3pd)	13.8	1.3	1.1	55.6	29.0	7.0	7.3	4.6	−37.4	59.9
6-311++G(3df,3pd)	11.4	0.9	0.8	86.4	21.2	3.7	6.7	4.1	7.2	48.1
cc-pVDZ	−41.3	−6.8	−6.3	0.5	−18.7	−64.8	−7.9	−8.1	−104.5	−9.5
aug-cc-pVDZ	−38.2	−8.9	−7.6	103.2	−17.7	−73.8	−10.6	−10.2	30.6	5.3
cc-pVTZ	4.4	−0.6	−0.5	82.5	5.9	−6.0	4.9	2.5	8.2	19.4
aug-cc-pVTZ	4.7	−0.9	−0.7	99.7	9.0					
CCSD/cc-pVDZ	−56.4	−15.0	−12.2	−101.9	−4.0					
CAM-B3LYP-D3BJ						**ωB97X-D**				
6-311G(d,p)	22.1	2.2	2.1	36.9	−20.7	15.1	−1.5	−0.5	39.1	−26.1
6-311++G(d,p)	21.7	0.6	1.1	83.3	−36.0	14.9	−0.1	0.4	5.4	−22.5
cc-pVDZ	−3.4	−0.9	−0.9	−16.7	−24.9	−9.1	−3.4	−2.7	−32.6	−19.2
aug-cc-pVDZ	−0.3	−3.1	−2.2	80.0	−24.8	−6.6	−5.2	−3.8	21.4	−17.3
cc-pVTZ	42.0	5.4	5.0	57.0	0.2	35.3	2.9	3.1	13.0	2.4
aug-cc-pVTZ	42.3	5.0	4.8	73.5	1.3	35.7	2.7	3.0	18.7	2.8
Experiment	3447.6	927.0	737.5	301.8	157.3					

no top–top coupling, we expected no interaction between the acetyl methyl and the ring methyl groups.

3. Microwave spectroscopy

A molecular jet Fourier-transform microwave spectrometer operating in the frequency range of 2.0 to 26.5 GHz[58] was used to record the spectrum of 2A5MT. The substance was purchased from TCI Europe, Zwijndrecht, Belgium, with a stated purity of >96.0% and used without further purification. Since 2A5MT is solid at room temperature with a melting point between 27 and 28 °C, we first heated the sample until the substance became liquid, and then added a few drops on a 5 cm piece of pipe cleaner. The pipe cleaner was placed in a metal tube upstream the nozzle heated to about 40 °C during measurements. Helium was flown as a carrier gas over the sample with a backing pressure of about 2 bar to transport the substance into the cavity.

Unlike in many of our investigations, no broadband scan was recorded for 2A5MT. Instead, an approach similar to the investigation of 2-ethylfuran[59] was employed. We only recorded very small scan portions of about 40 to 300 MHz around the predicted frequencies of some transitions with the highest expected intensities. This was only possible with the results from previous benchmarks for the isomers 2A3MT[23] and 2A4MT,[24] showing that the B_e rotational constants calculated at the MP2/6-31G(d,p) level of theory are very close to the experimentally determined B_0 values. Therefore, the spectrum of the more stable conformer *syn*-2A5MT was first predicted with the program XIAM[18] using the values obtained at this level (see Table 1). The first transition that we searched for, $5_{15} \leftarrow 4_{04}$, was predicted at 9568.69 MHz, and we started the scan at 9532 MHz as a series of overlapping spectra with a step width of 0.25 MHz. We observed three strong lines very close to the expected frequency at 9569.25 MHz, 9573.25 MHz, and 9576.5 MHz, which were subsequently remeasured at a higher resolution with an experimental accuracy of 2 kHz.[60] All three lines appear as Doppler pairs in the high resolution measurements due to the co-axial arrangement between the molecular beam and the resonator. They are three of the five torsional species expected for a two-top molecule. For torsional barriers of 165.5 and 359.0 cm^{-1} (see Fig. 3), the (00) and (01) species often appear as a doublet and the (10), (11) and (12) species appear as a triplet. Therefore, we suspected the three observed

512 | *Phys. Chem. Chem. Phys.*, 2023, **25**, 509–519

This journal is © the Owner Societies 2023
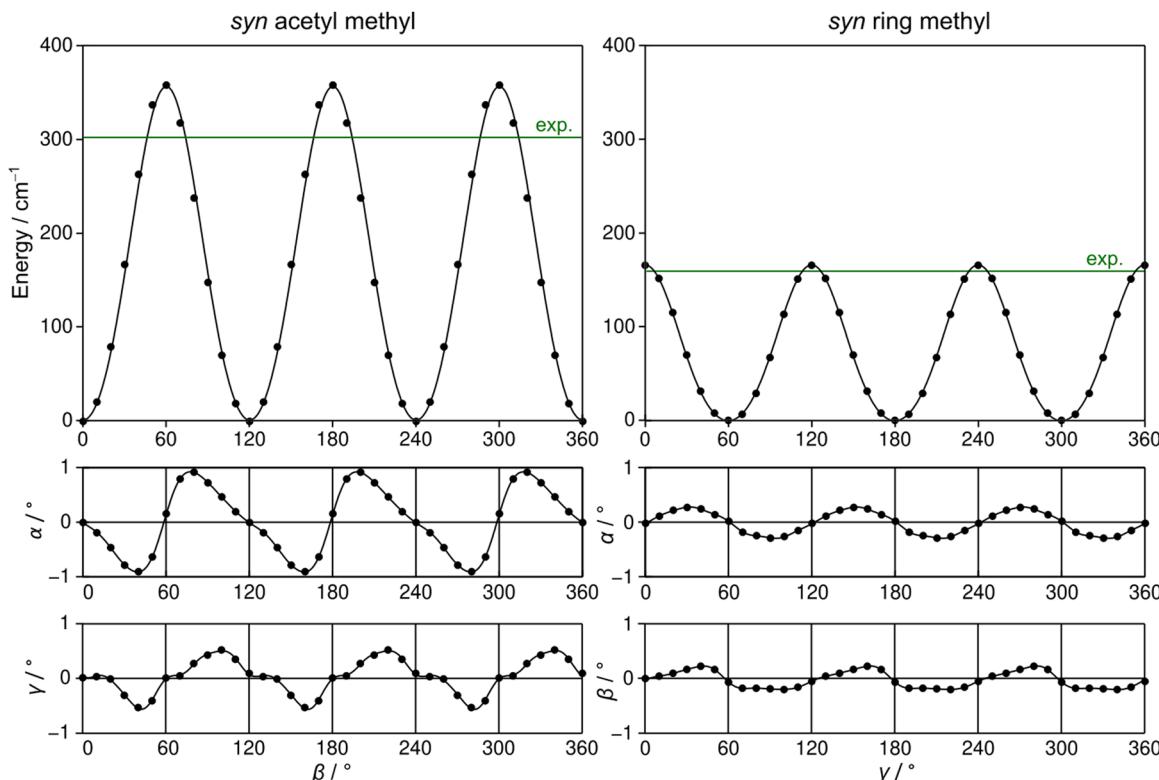
Fig. 3 Left hand side: The potential energy curve of *syn*-2A5MT obtained at the MP2/6-31G(d,p) level of theory by rotating the acetyl methyl group about the C6–C8 bond by varying the dihedral angle β in steps of 10°. The energies are given relative to the lowest energy with $E = -743.3683071$ hartree. The calculated barrier height is 359.0 cm^{-1}. The middle trace visualises the oscillation of the acetyl group upon the acetyl methyl rotation and the lowest trace that of the ring methyl group. The deviations of the dihedral angles α and γ are given relative to the values of the fully optimised geometries, which are 0.00° for α and 179.86° for γ. Right hand side: The potential energy curve of *syn*-2A5MT obtained by rotating the ring methyl group about the C5–C9 bond by varying the dihedral angle γ in steps of 10°. The energies are given relative to the lowest energy with $E = -743.3683069$ hartree. The calculated barrier height is 165.5 cm^{-1}. The middle trace visualises the oscillation of the acetyl group upon the ring methyl rotation and the lowest trace that of the acetyl methyl group. The deviations of the dihedral angles α and β are given relative to the values of the fully optimised geometries, which are 0.00° for both α and β.
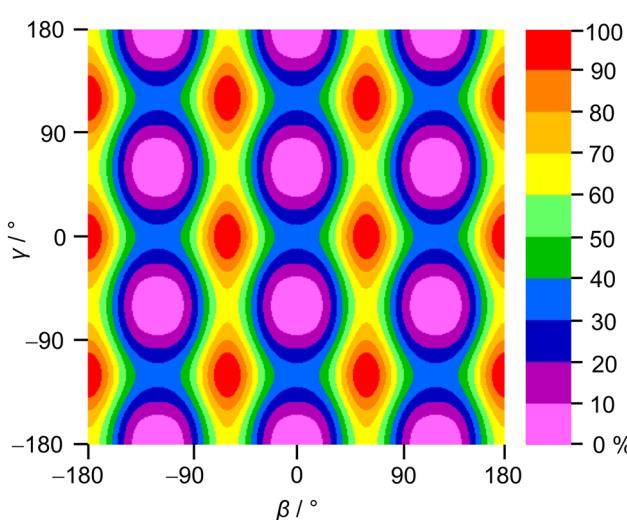
Fig. 4 Two-dimensional potential energy surface of *syn*-2A5MT calculated at the MP2/6-31G(d,p) level of theory in dependence of the dihedral angles β and γ, which were varied in a grid of 10° while all other geometry parameters were optimised. The colour code gives the relative energy (in percent) on a scale between the minimum $E_{min} = -743.368307$ hartree (0%) and the maximum $E_{max} = -743.365928$ hartree (100%).

lines to be the (10), (11) and (12) species of the $5_{15} \leftarrow 4_{04}$ transition, although an assignment was not yet possible at this point.

Similarly, we searched for the $6_{16} \leftarrow 5_{05}$ and $7_{17} \leftarrow 6_{06}$ transitions and found the triplets red shifted from the predicted frequencies by less than 30 MHz. Further intense triplets could be found easily afterwards. The identification of all five torsional species was finally possible with the observation of quintets for the *a*-type *R*-branch $6_{16} \leftarrow 5_{15}$, $7_{17} \leftarrow 6_{16}$, $8_{18} \leftarrow 7_{17}$ due to the relatively small splittings between the species as shown in Fig. 5. We could then establish a first fit with the program XIAM which only incorporates the (00) species. This (00) fit was rapidly expanded with the (01) and (10) species into two separate one rotor fits and finally into a two-top fit taking all five torsional species into account. At this stage, transitions could be predicted with an accuracy of about 3 kHz, measured, and added to the fit. Ultimately, 427 transitions were included in a two-top fit shown in Table 3 with a standard deviation of 2.9 kHz. The standard deviation is very close to the estimated measurement accuracy of 2.7 kHz, corresponding to 1/10th of the average line width at half height (FWHH) of 27 kHz. The assigned transition frequencies are listed in Table S6 in the ESI.† All scan portions measured between 8000 and 14 000 MHz

This journal is © the Owner Societies 2023

Phys. Chem. Chem. Phys., 2023, **25**, 509–519 | **513**
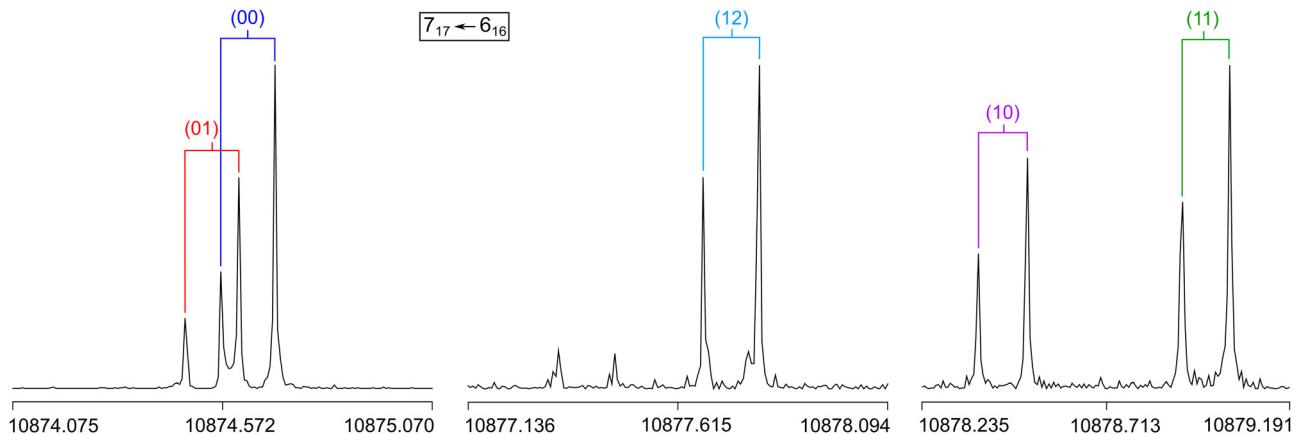
Fig. 5 High resolution measurements of the a-type transition $7_{17} \leftarrow 6_{16}$ with its five torsional species (00), (10), (01), (11), and (12). The frequencies are in MHz. The brackets indicate Doppler pairs. The spectra were recorded at 10 874.75 MHz and 10 877.75 MHz with 50 co-added free induction decays (FIDs), and at 10 878.97 MHz with 116 co-added FIDs.

Table 3 Experimental spectroscopic parameters of syn-2A5MT obtained with the program XIAM compared to the predicted values. Top 1 refers to the acetyl methyl group and top 2 refers to the ring methyl group

Par.[a]	Unit	XIAM	MP2[b]
A_0	MHz	3447.62273(27)	3406.116
B_0	MHz	927.022235(89)	922.127
C_0	MHz	737.533474(35)	732.579
Δ_J	kHz	0.02132(36)	0.0200
Δ_{JK}	kHz	—	−0.0015
Δ_K	kHz	0.3161(94)	0.3279
δ_J	kHz	0.00472(17)	0.0046
δ_K	kHz	0.0385(93)	0.0330
$V_{3,1}$	cm^{-1}	301.811(41)	359.0
$D_{p_i^2 J,1}$	kHz	18.33(59)	
$D_{p_i^2 K,1}$	kHz	−214.6(51)	
$D_{p_i^2 -,1}$	kHz	8.36(61)	
$\angle(i_1,a)$	°	44.338(31)	47.9
$\angle(i_1,b)$	°	45.661(31)	42.1
$\angle(i_1,c)$	°	90.0^c	90.0
$V_{3,2}$	cm^{-1}	157.2612(13)	165.5
$D_{p_i^2 J,2}$	kHz	−3.641(63)	
$D_{p_i^2 K,2}$	kHz	165.64(55)	
$D_{p_i^2 -,2}$	kHz	0.775(67)	
$\angle(i_2,a)$	°	16.2798(39)	16.6
$\angle(i_2,b)$	°	73.7202(39)	73.4
$\angle(i_2,c)$	°	90.0^c	90.0
N^d		427	
σ^e	kHz	2.9	

^{a} All parameters refer to the principal axis system. Watson's A reduction and I^r representation were used. ^{b} Calculated with the 6-31G(d,p) basis set. The ground state rotational constants and centrifugal distortion constants obtained from anharmonic frequency calculations are given. ^{c} Fixed due to symmetry. ^{d} Number of transitions. ^{e} Standard deviation of the fit.

Fig. 6 Partial scans between 8 and 14 GHz of 2A5MT. The experimental spectrum is shown in the upper trace. The lower trace displays the theoretical spectrum of syn-2A5MT predicted using the molecular parameters obtained from the fit given in Table 3. The grey sections were not scanned. The five torsional species are colour-coded according to Fig. 5.

very weak lines that potentially belong to $anti$-2A5MT, even while using a higher number of 200 co-added decays per measurement to consider that $anti$-2A5MT is higher in energy than syn-2A5MT and may possess lines with a lower intensity.

4. Discussion

4.1 Conformational stability

Only the most stable of the two expected conformers was observed in the microwave spectrum of 2A5MT, confirming the higher energetic stability predicted for the syn form compared to the $anti$-form. The preference for the syn-conformer has already been established in other thiophene derivatives such as 2-thiophenecarboxaldehyde,[61,62] 2-acetylthiophene,[45] and the isomer 2A4MT[24] of 2A5MT. This was explained due to dipole–dipole interactions between the positively charged sulphur atom in the thiophene ring and the negatively charged oxygen of the carbonyl group,[24,45,61] which also holds true for 2A5MT, as shown in the

and the fitted spectrum of syn-2A5MT are shown in Fig. 6. The rotational barriers of the acetyl methyl and the ring methyl groups were experimentally determined to be 301.811(41) cm^{-1} and 157.2612(13) cm^{-1}, respectively. The parameters $F_{0,1}$ and $F_{0,2}$, describing the moments of inertia of the two methyl internal rotors, could not be fitted and were fixed to 158 GHz, a value often found for methyl groups.

Finally, we attempted to assign the $anti$-conformer of 2A5MT in the same manner as syn-2A5MT. However, we only found two

514 | $Phys. Chem. Chem. Phys.$, 2023, **25**, 509–519

This journal is © the Owner Societies 2023

Fig. 7 Charge distribution in *syn*- and *anti*-2A5MT obtained from NBO calculations at the MP2/6-31G(d,p) level of theory.

results of the NBO calculations[63] given in Fig. 7. The only exception of thiophene derivatives where the *anti*-conformer is more stable is the isomer 2A3MT[23] of 2A5MT due to steric interactions between the ring methyl group and the acetyl group.[36]

In our previous investigations on thiophene derivatives,[23,24,45,64] we often observed discrepancies while calculating the molecular structures at different levels of theory concerning the planarity. A number of MP2 calculations predicted the molecules to be non-planar due to an out-of-plane tilt of the acetyl group. In the case of *syn*-2A5MT, only the MP2/6-311++G(df,pd) level predicts a non-planar structure with a small tilt angle of about 3°; all other employed levels agree on a planar structure. Together with the inertial defect of 6.523 uÅ^2, which is close to those of other planar molecules with four out-of-plane hydrogen atoms such as the *cis–trans* conformer of ethylnitrite ($\Delta_c = -6.422$ uÅ^2)[65] and the C_s conformer of 2-ethylfuran ($\Delta_c = -6.483$ uÅ^2),[59] the planarity question does not arise for *syn*-2A5MT.

4.2 Benchmarking 2-acetylthiophenes

The XIAM fit given in Table 3 includes 451 lines and reaches a standard deviation of 2.9 kHz, satisfactorily close to the measurement accuracy of 2.7 kHz. All the rotational and centrifugal distortion constants, except Δ_{JK} which was finally not fitted, and the internal rotation parameters were determined with high accuracy.

It is known that a comparison between the calculated rotational constants B_e and the experimentally determined ones B_0 is physically not meaningful, as the former refers to the equilibrium structure and the latter to the vibrational ground state. Nevertheless, our benchmarking efforts given in Section 2 are still helpful to determine the level of theory which deliver B_e values close to the experimental ones. Even though this agreement is due to error compensations, this allows rapid spectral assignments of related molecules in future studies, as shown in the present case of 2A5MT. From the benchmarks carried out for 2A3MT[23] and 2A4MT,[24] we could significantly reduce the measurement time of 2A5MT by using B_e rotational constants predicted at the MP2/6-31G(d,p) level of theory to guide the assignments. The benchmarking of *syn*-2A5MT shows that the B and C constants were predicted very accurately with deviations less than 1 MHz, but a larger deviation was found for the A constant (see Table 2 and Table S3, ESI†), though the difference is still quite acceptable. The values closest to the experimental

ones were provided by the M06-2X/6-31G(d,p) level of theory. We note that the Pople's basis set 6-31G(d,p) is also involved here. Good results were also achieved when diffusion functions +(+) are added, as well as at the B3LYP-D3BJ/6-311(+)G(2d,2p) levels of theory that also performed very well for 2A3MT.[23]

The torsional barriers of the ring methyl group and the acetyl methyl group of *syn*-2A5MT were determined to be 301.811(41) cm^{-1} and 157.2612(13) cm^{-1}, respectively. Compared to the calculated values (see Table 2 and Table S3, ESI†), the predictions are not very accurate, though generally the ring methyl barrier was better predicted than the acetyl methyl barrier. Currently, there are no obvious trends regarding methods or basis sets that can be recommended, except the few following points: (1) for the B3LYP method, either with D3 or D3BJ corrections or in the CAM-B3LYP variation, adding diffusion functions decreases the accuracy of calculations for the acetyl methyl group but not for the ring methyl group. (2) In most cases, adding Becke-Johnson damping decreases the accuracy of calculations for both methyl groups. (3) For the MP2, M06-2X and ωB97X-D methods, adding diffusion functions increases the accuracy of calculations for the acetyl methyl group. For the ring methyl group, there is no clear trend. Therefore, we only note two levels of theory, MP2/6-311+G(d,p) and B3LYP-D3/6-311G(2df,2dp), which predict values with less than 10 cm^{-1} deviation from the experimental value for both rotors. These two levels also perform well for the acetyl methyl rotors of 2A3MT[23] and 2A4MT.[24]

4.3 Barriers to methyl internal rotations

Aromatic rings are of special interest while coupled with multiple methyl internal rotors as the conjugated double bond system is able to transfer electrostatic effects over a longer distance through the π-electrons, making the barrier to methyl torsion sometimes unpredictable.[36] Heterocycles such as thiophene and furan additionally have the influence of the heteroatom on the torsional barrier. It was shown in the literature that changing from sulphur to oxygen increases the barrier, *i.e.*, dimethyl sulfide (736 cm^{-1})[66] *vs.* dimethyl ether (944 cm^{-1}),[67] *trans*-ethyl methyl sulfide (693 cm^{-1})[68] *vs.* *trans*-ethyl methyl ether (893 cm^{-1}),[69] conformer III of *n*-propyl sulfide (699 cm^{-1})[70] *vs.* *trans–trans*-methyl-*n*-propyl ether (1154 cm^{-1}),[71] and *S*-phenyl thioacetate (48 cm^{-1})[72] *vs.* phenyl acetate (137 cm^{-1}).[34] The same holds true for all methyl rotors attached to the thiophene and furan rings illustrated in Fig. 8, but interestingly not for the acetyl

This journal is © the Owner Societies 2023

Phys. Chem. Chem. Phys., 2023, **25**, 509–519 | **515**

methyl rotors. Only two sulphur/oxygen analogue pairs possessing an acetyl methyl rotor have been studied so far, 2-acetylthiophene (molecule (**1**) in Fig. 8)[45] and 2-acetylfuran (**5**)[73] as well as *syn*-2A5MT (**11**) and 2-acetyl-5-methylfuran (**12**),[74] where the lower torsional barrier of the acetyl methyl group was observed for the *syn*-conformers of furans. The question of why only the acetyl methyl group of the *syn* conformers and not of the *anti*-ones shows this different behaviour, is still lacking an answer. To better understand this phenomenon, investigations on 2-acetyl-3-methylfuran and 2-acetyl-4-methylfuran, as well as the 3-acetylmethylthiophene isomers would be helpful and interesting.

The various thiophenes and furans shown in Fig. 8 possess either a ring methyl group, an acetyl methyl group, or both. The influence of electrostatic effects can be shown by comparing the barriers in 2-methylthiophene (**2**) (194.1 cm^{-1})[75] and 2,5-dimethylthiophene (**4**) (248.0 cm^{-1})[77] as well as in their oxygen analogues 2-methylfuran (**6**) (412.9 cm^{-1})[78] and 2,5-dimethylfuran (**8**) (439.1 cm^{-1}).[80] The presence of a second methyl group causes

an increase of the torsional barrier in both cases. As the methyl groups at the 2- and the 5-positions cannot interact by steric effects, electrostatic effects have to be the reason. The comparison of the ring methyl barriers in *syn*-2A5MT (**11**) (157.3 cm^{-1}) and 2-methylthiophene (**2**) (194.1 cm^{-1})[75] demonstrates that the negative inductive and mesomeric effects of the carbonyl group decrease the methyl torsional barrier. Only in *anti*-2A3MT (**9**),[23] the presence of an acetyl substituent increases the barrier to 321.8 cm^{-1} compared to the value of 258.8 cm^{-1} found for 3-methylthiophene (**3**).[76] The reason was steric hindrance between the acetyl group at the second substitution position and the methyl group at the third substitution position. The barrier of the ring methyl rotor is independent of the orientation of the acetyl group, as demonstrated by the almost unchanged value found for *syn*-2A4MT (**10a**) (210.7 cm^{-1}) and *anti*-2A4MT (**10b**) (213.0 cm^{-1}).[24]

The ring methyl group also affects the barrier to the internal rotation of the acetyl methyl group. Comparing the values
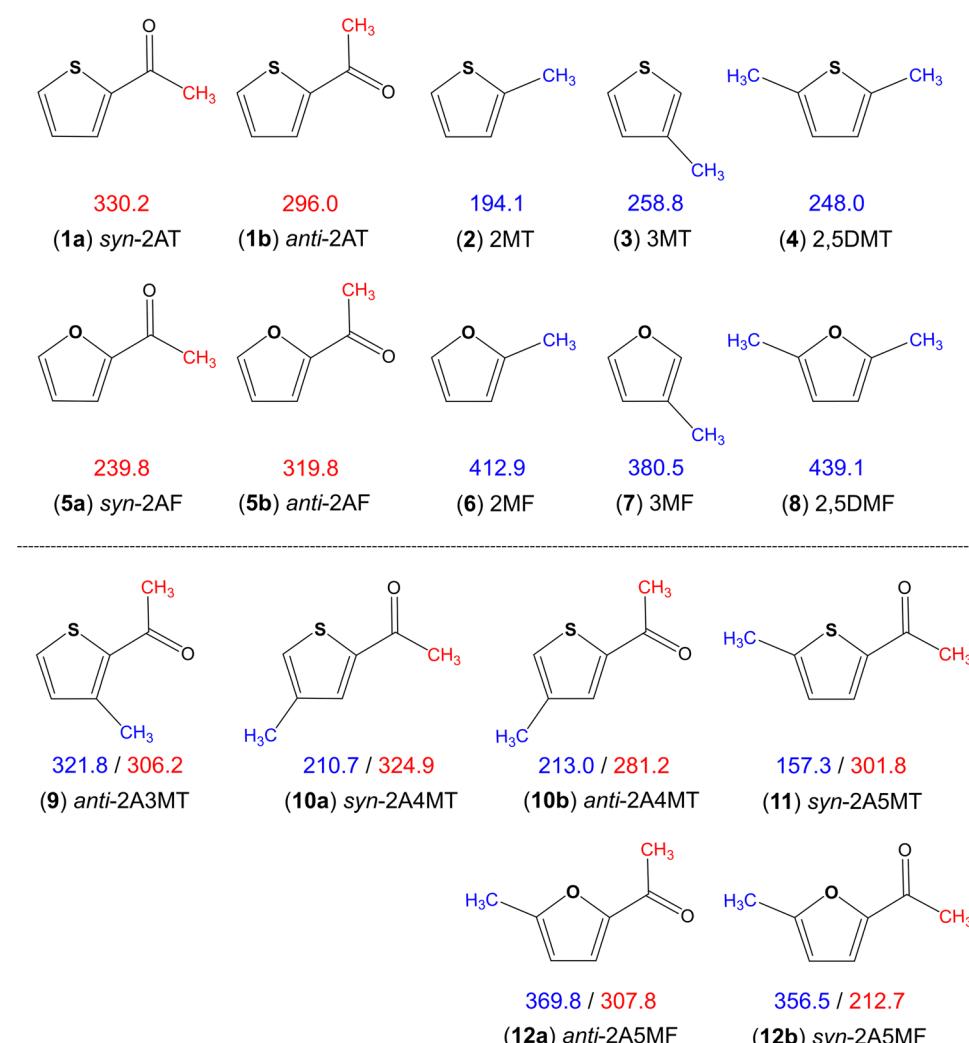
Fig. 8 Comparison of barriers to internal rotations (in cm^{-1}) of the acetyl (red) and ring (blue) methyl groups in thiophene and furan derivatives: (**1**) 2-acetylthiophene,[45] (**2**) 2-methylthiophene,[75] (**3**) 3-methylthiophene,[76] (**4**) 2,5-dimethylthiophene,[77] (**5**) 2-acetylfuran,[73] (**6**) 2-methylfuran,[78] (**7**) 3-methylfuran,[79] (**8**) 2,5-dimethylfuran,[80] (**9**) *anti*-2-acetyl-3-methylthiophene,[23] (**10**) 2-acetyl-4-methylthiophene,[24] (**11**) *syn*-2-acetyl-5-methylthiophene (this work) and (**12**) 2-acetyl-5-methylfuran.[74]

516 | *Phys. Chem. Chem. Phys.*, 2023, **25**, 509–519

This journal is © the Owner Societies 2023

observed for *anti*-2-acetylthiophene (**1b**) (296.0 cm^{-1}) and *syn*-2-acetylthiophene (**1a**) (330.2 cm^{-1}) to those of 2A3MT (**9**), 2A4MT (**10**) and 2A5MT (**11**), we found that the barrier decreases with the presence of a methyl group on the thiophene ring at the 4- or the 5-position,[24] but increases if the methyl group is at the 3-position.[23] The comparison between 2-acetylfuran (**5**)[73] and 2-acetyl-5-methylfuran (**12**)[74] leads to the same observation. In previous studies on a series of acetyl group containing linear aliphatic ketones, the chain-length effect has been introduced, stating that if the molecular shape is more prolate, the torsional barrier of the acetyl methyl group becomes lower.[37] This effect can explain the above-mentioned observation. The addition of a methyl group at the 4- and the 5-position of the thiophene ring makes the molecule more prolate compared to 2-acetylthiophene or 2-acetylfurane and decreases the barrier, while the addition of a methyl group at the 3-position makes the molecule more globular and increases the barrier.[36]

Overall, it is noticeable that the barriers of the acetyl methyl group fall into a much wider range for furan derivatives (212.7 cm^{-1} to 319.8 cm^{-1}) than that for thiophene derivatives (281.2 cm^{-1} to 330.2 cm^{-1}). In ref. 24, we proposed a "thiophene class", as an extension to the classification system proposed by Andresen *et al.*[37,38] and Herbers *et al.*[42] for the acetyl methyl torsional barrier. We found that the barrier heights of acetylthiophene derivatives are 300 cm^{-1}, and the present study on *syn*-2A5MT firmly supports this hypothesis.

5. Conclusion

Previous benchmarking efforts on similar molecules allowed for the very rapid assignment of the *syn*-conformer of 2A5MT where only small scan portions of the microwave spectrum were required. The barrier heights were determined for the two inequivalent rotors, the acetyl methyl and the ring methyl groups, to be 301.811(41) cm^{-1} and 157.2612(13) cm^{-1}, respectively. A comparison with other thiophene derivatives possessing either an acetyl group, a ring methyl group, or both indicates that electrostatic effects influencing the torsional barriers are transferred through the π-electron system of the heteroaromatic ring. It was also observed that the chain length effects reported for α,β-saturated ketones hold true for 2-acetylthiophene derivatives, *i.e.*, the more prolate the molecular frame, the lower the torsional barrier of the acetyl methyl rotor. The effect of the heteroatom in the ring on methyl torsion was also investigated by comparing the barrier heights in thiophene and furan derivatives. The usual observation that the torsional barrier is higher in oxygen analogues compared to that in equivalent sulphur analogues is no longer the case for the *syn*-conformers of 2-acetylfuran *vs.* 2-acetylthiophene and 2-acetyl-5-methylfuran *vs.* 2A5MT. The torsional barriers of acetyl methyl groups in molecules with a thiophene ring attached at the other side of the carbonyl bond are always around 300 cm^{-1} and can thus be grouped together in the so-called "thiophene class".

Conflicts of interest

There are no conflicts to declare.

Acknowledgements

References

1   H. H. Nielsen, *Phys. Rev.*, 1932, **40**, 445–456.
2   J. D. Kemp and K. S. Pitzer, *J. Chem. Phys.*, 1936, **4**, 749–750.
3   A. M. Halpern and E. D. Glendening, *J. Chem. Phys.*, 2003, **119**, 11186–11191.
4   V. Pophristic and L. Goodman, *Nature*, 2001, **411**, 565–586.
5   R. F. W. Bader, J. R. Cheeseman, K. E. Laidig, K. B. Wiberg and C. Breneman, *J. Am. Chem. Soc.*, 1990, **112**, 6530–6536.
6   T. Kundu, B. Pradhan and B. P. Singh, *J. Chem. Sci.*, 2002, **114**, 623–638.
7   S. Liu, N. Govind and L. G. Pedersen, *J. Chem. Phys.*, 2008, **129**, 094104.
8   D. G. Lister, J. N. Macdonald and N. L. Owen, *Internal Rotation and Inversion*, Academic Press, London, 1978.
9   H. V. L. Nguyen and I. Kleiner, *Phys. Sci. Rev.*, 2022, **7**, 679–726.
10 J.-U. Grabow, Fourier Transform Microwave Spectroscopy Measurement and Instrumentation. in *Handbook of High-Resolution Spectroscopy*, ed. M. Quack and F. Merkt, Wiley, Chichester, UK, 2011, ch. 1, vol. 2.
11 J. T. Hougen, I. Kleiner and M. Godefroid, *J. Mol. Spectrosc.*, 1994, **163**, 559–586.
12 I. Kleiner and J. T. Hougen, *J. Chem. Phys.*, 2003, **119**, 5505–5509.
13 V. V. Ilyushin, Z. Kisiel, L. Pszczolkowski, H. Mäder and J. T. Hougen, *J. Mol. Spectrosc.*, 2010, **259**, 26–38.
14 L. Ferres, W. Stahl and H. V. L. Nguyen, *J. Chem. Phys.*, 2018, **148**, 124304.
15 P. Groner, *J. Chem. Phys.*, 1997, **107**, 4483–4498.
16 M. Tudorie, I. Kleiner, J. T. Hougen, S. Melandri, L. W. Sutikdja and W. Stahl, *J. Mol. Spectrosc.*, 2011, **269**, 211–225.
17 V. V. Ilyushin and J. T. Hougen, *J. Mol. Spectrosc.*, 2013, **289**, 41–49.
18 H. Hartwig and H. Dreizler, *Z. Naturforsch.*, 1996, **51a**, 923–932.
19 L. Ferres, W. Stahl and H. V. L. Nguyen, *J. Chem. Phys.*, 2019, **151**, 104310.
20 L. Ferres, J. Cheung, W. Stahl and H. V. L. Nguyen, *J. Phys. Chem. A*, 2019, **123**, 3497–3503.
21 P. R. Bunker and P. Jensen, *Molecular Symmetry and Spectroscopy*, NRC Research Press, Ottawa, Ontario, Canada, 2nd edn, 2006.
22 H. Dreizler, *Z. Naturforsch.*, 1961, **16a**, 1354–1367.
23 C. Dindić and H. V. L. Nguyen, *Chem. Phys. Chem.*, 2021, **22**, 2420–2428.

This journal is © the Owner Societies 2023

Phys. Chem. Chem. Phys., 2023, **25**, 509–519 | **517**

24 C. Dindić, M. Barth and H. V. L. Nguyen, *Spectrochim. Acta, Part A*, 2022, **280**, 121505.

25 S. Khemissi, A. Pérez Salvador and H. V. L. Nguyen, *J. Phys. Chem. A*, 2021, **125**, 8542–8548.

26 K. P. R. Nair, S. Herbers, J.-U. Grabow and H. V. L. Nguyen, *J. Mol. Struct.*, 2021, **1246**, 131096.

27 J. Mélan, S. Khemissi and H. V. L. Nguyen, *Spectrochim. Acta, Part A*, 2021, **253**, 119564.

28 K. Eibl, W. Stahl, I. Kleiner and H. V. L. Nguyen, *J. Chem. Phys.*, 2018, **149**, 144306.

29 L. Sutikdja, W. Stahl, V. Sironneau, H. V. L. Nguyen and I. Kleiner, *Chem. Phys. Lett.*, 2016, **663**, 145–149.

30 T. Attig, R. Kannengießer, I. Kleiner and W. Stahl, *J. Mol. Spectrosc.*, 2014, **298**, 47–53.

31 H. V. L. Nguyen, A. Jabri, V. Van and W. Stahl, *J. Phys. Chem. A*, 2014, **118**, 12130–12136.

32 A. Jabri, V. Van, H. V. L. Nguyen, W. Stahl and I. Kleiner, *Chem. Phys. Chem.*, 2016, **17**, 2660–2665.

33 H. V. L. Nguyen and W. Stahl, *J. Mol. Spectrosc.*, 2010, **264**, 120–124.

34 L. Ferres, L. Evangelisti, A. Maris, S. Melandri, W. Caminati, W. Stahl and H. V. L. Nguyen, *Molecules*, 2022, **27**, 2730.

35 Y. Zhao, H. Mouhib, G. Li, I. Kleiner and W. Stahl, *J. Mol. Spectrosc.*, 2016, **322**, 38–42.

36 H. V. L. Nguyen, W. Caminati and J.-U. Grabow, *Molecules*, 2022, **27**, 3948.

37 M. Andresen, D. Schöngen, I. Kleiner, M. Schwell, W. Stahl and H. V. L. Nguyen, *Chem. Phys. Chem.*, 2020, **21**, 2206–2216.

38 M. Andresen, M. Schwell and H. V. L. Nguyen, *J. Mol. Struct.*, 2022, **1247**, 131337.

39 M. Andresen, I. Kleiner, M. Schwell, W. Stahl and H. V. L. Nguyen, *J. Phys. Chem. A*, 2018, **122**, 7071–7078.

40 M. Andresen, I. Kleiner, M. Schwell, W. Stahl and H. V. L. Nguyen, *Chem. Phys. Chem.*, 2019, **20**, 2063–2073.

41 M. Andresen, I. Kleiner, M. Schwell, W. Stahl and H. V. L. Nguyen, *J. Phys. Chem. A*, 2020, **124**, 1353–1361.

42 S. Herbers, S. M. Fritz, P. Mishra, H. V. L. Nguyen and T. S. Zwier, *J. Chem. Phys.*, 2020, **152**, 074301.

43 K. G. Lengsfeld: *Van-der-Waals-Wechselwirkungen: Präzise Struktur und Dynamik von Molekülen*, PhD thesis, Gottfried Wilhelm Leibniz Universität Hannover, 2022.

44 V. L. Orr, Y. Ichikawa, A. R. Patel, A. M. Kougias, K. Kobayashi, J. F. Stanton, B. J. Esselman, R. C. Woods and R. J. McMahon, *J. Chem. Phys.*, 2021, **154**, 244310.

45 C. Dindić, J. Ludovicy, V. Terzi, A. Lüchow, N. Vogt, J. Demaison and H. V. L. Nguyen, *Phys. Chem. Chem. Phys.*, 2022, **24**, 3804–3815.

46 C. Møller and M. S. Plesset, *Phys. Rev.*, 1934, **46**, 618–622.

47 M. J. Frisch, J. A. Pople and J. S. Binkley, *J. Chem. Phys.*, 1984, **80**, 3265–3269.

48 M. J. Frisch, G. W. Trucks, H. B. Schlegel, G. E. Scuseria, M. A. Robb, J. R. Cheeseman, G. Scalmani, V. Barone, G. A. Petersson, H. Nakatsuji, X. Li, M. Caricato, A. V. Marenich, J. Bloino, B. G. Janesko, R. Gomperts, B. Mennucci, H. P. Hratchian, J. V. Ortiz, A. F. Izmaylov, J. L. Sonnenberg, D. Williams-Young, F. Ding, F. Lipparini, F. Egidi, J. Goings, B. Peng, A. Petrone, T. Henderson, D. Ranasinghe, V. G. Zakrzewski, J. Gao, N. Rega, G. Zheng, W. Liang, M. Hada, M. Ehara, K. Toyota, R. Fukuda, J. Hasegawa, M. Ishida, T. Nakajima, Y. Honda, O. Kitao, H. Nakai, T. Vreven, K. Throssell, J. A. Montgomery, Jr., J. E. Peralta, F. Ogliaro, M. J. Bearpark, J. J. Heyd, E. N. Brothers, K. N. Kudin, V. N. Staroverov, T. A. Keith, R. Kobayashi, J. Normand, K. Raghavachari, A. P. Rendell, J. C. Burant, S. S. Iyengar, J. Tomasi, M. Cossi, J. M. Millam, M. Klene, C. Adamo, R. Cammi, J. W. Ochterski, R. L. Martin, K. Morokuma, O. Farkas, J. B. Foresman and D. J. Fox, *Gaussian 16, Revision B.01*, Gaussian, Inc., Wallingford CT, 2016.

49 A. D. Becke, *J. Chem. Phys.*, 1993, **98**, 5648–5652.

50 C. Lee, W. Yang and R. G. Paar, *Phys. Rev. B: Condens. Matter Mater. Phys.*, 1988, **37**, 785–789.

51 S. Grimme, J. Antony, S. Ehrlich and H. Krieg, *J. Chem. Phys.*, 2010, **132**, 154104.

52 S. Grimme, S. Ehrlich and L. Goerigk, *J. Comput. Chem.*, 2011, **32**, 1456–1465.

53 T. Yanai, D. P. Tew and N. C. Handy, *Chem. Phys. Lett.*, 2004, **393**, 51–57.

54 Y. Zhao and D. G. Truhlar, *Theor. Chem. Acc.*, 2008, **120**, 215–241.

55 J.-D. Chai and M. Head-Gordon, *Phys. Chem. Chem. Phys.*, 2008, **10**, 6615–6620.

56 G. E. Scuseria, A. C. Scheiner, T. J. Lee, J. E. Rice and H. F. Schaefer III, *J. Chem. Phys.*, 1987, **86**, 2881–2890.

57 T. H. Dunning Jr., *J. Chem. Phys.*, 1989, **90**, 1007–1023.

58 J.-U. Grabow, W. Stahl and H. Dreizler, *Rev. Sci. Instrum.*, 1996, **67**, 4072–4084.

59 H. V. L. Nguyen, *J. Mol. Struct.*, 2020, **1208**, 127909.

60 J.-U. Grabow and W. Stahl, *Z. Naturforsch.*, 1990, **45a**, 1043–1044.

61 R. Hakiri, N. Derbel, W. C. Bailey, H. V. L. Nguyen and H. Mouhib, *Mol. Phys.*, 2020, **118**, e1728406.

62 W. Li, M. Li, Y. Jan, Q. Gou, J.-U. Grabow and G. Feng, *J. Chem. Phys.*, 2019, **151**, 164307.

63 E. D. Glendening, C. R. Landis and F. Weinhold, *Wiley Interdisc. Rev.: Comput. Mol. Sci.*, 2012, **2**, 1–42.

64 C. Dindić, W. Stahl and H. V. L. Nguyen, *Phys. Chem. Chem. Phys.*, 2020, **22**, 19704.

65 N. Hansen, F. Temps, H. Mäder and N. W. Larsen, *Phys. Chem. Chem. Phys.*, 1999, **1**, 3219–3233.

66 A. Jabri, V. Van, H. V. L. Nguyen, H. Mouhib, F. Kwabia Tchana, L. Manceron, W. Stahl and I. Kleiner, *Astron. Astrophys.*, 2016, **589**, A127.

67 W. Neustock, A. Guarnieri, J. Demaison and G. Wlodarczak, *Z. Naturforsch.*, 1990, **45a**, 702–706.

68 M. Hayashi, M. Adachi and J. Nakagawa, *J. Mol. Spectrosc.*, 1981, **86**, 129–135.

69 M. Hayashi and K. Kuwada, *J. Mol. Struct.*, 1975, **28**, 147–161.

70 L. Tulimat, H. Mouhib, H. V. L. Nguyen and W. Stahl, *J. Mol. Spectrosc.*, 2020, **373**, 111356.

71 H. Kato, J. Nakagawa and M. Hayashi, *J. Mol. Spectrosc.*, 1980, **80**, 272–278.

518 | *Phys. Chem. Chem. Phys.*, 2023, **25**, 509–519

This journal is © the Owner Societies 2023

72 L. Ferres, *Quantum Chemical and Microwave Spectroscopic Investigations on Phenyl Ring Containing Molecules*, PhD thesis, RWTH Aachen University, 2019.

73 C. Dindić, A. Lüchow, N. Vogt, J. Demaison and H. V. L. Nguyen, *J. Phys. Chem. A*, 2021, **125**, 4986–4997.

74 V. Van, W. Stahl and H. V. L. Nguyen, *Chem. Phys. Chem.*, 2016, **17**, 3223–3228.

75 N. M. Posdeev, L. N. Gunderova and A. A. Shapkin, *Opt. Spektrosk.*, 1970, **28**, 254.

76 T. Ogata and K. Kozima, *J. Mol. Spectrosc.*, 1972, **42**, 38–46.

77 V. Van, W. Stahl and H. V. L. Nguyen, *Phys. Chem. Chem. Phys.*, 2015, **17**, 32111–32114.

78 I. A. Finneran, S. T. Shipman and S. L. Widicus Weaver, *J. Mol. Spectrosc.*, 2012, **280**, 27–33.

79 T. Ogata and K. Kozima, *Bull. Chem. Soc. Jpn.*, 1971, **44**, 2344–2346.

80 V. Van, J. Bruckhuisen, W. Stahl, V. Ilyushin and H. V. L. Nguyen, *J. Mol. Spectrosc.*, 2018, **343**, 121–125.